JOURNAL OF GUIDANCE, CONTROL, AND DYNAMICS
Vol. 17, No. 4, July–August 1994

Design of Nonlinear Control Laws for High-Angle-of-Attack Flight

Richard J. Adams,* James M. Buffington,† and Siva S. Banda‡
Flight Dynamics Directorate, Wright-Patterson Air Force Base, Ohio 45433-7531

High-angle-of-attack flight control laws are developed for a supermaneuverable fighter aircraft. The methods of dynamic inversion and structured singular value synthesis are combined into an approach which addresses both the nonlinearity and robustness problems of flight at extreme operating conditions. The primary purpose of the dynamic inversion control elements is to linearize the vehicle response across the flight envelope. Structured singular value synthesis is used to design a dynamic controller which provides robust tracking to pilot commands. The resulting control system achieves desired flying qualities and guarantees a large margin of robustness to uncertainties for high-angle-of-attack flight conditions. High-fidelity nonlinear simulation results show that the combined dynamic inversion/structured singular value synthesis control law achieves a high level of performance in a realistic environment.

Introduction

SUPERMANEUVERABILITY is defined as the ability to maneuver an aircraft up to and beyond the stall angle of attack. Some tactical payoffs of high-angle-of-attack maneuvering include superior survivability, confusion of adversary pilots, and the ability to increase first-shot opportunities.[1] Additional control power in the form of forebody vortex flow control and thrust vectoring can allow fighter aircraft to operate in the poststall flight regime. Therefore, advanced control law design techniques must be found for robust high-angle-of-attack stability augmentation and maneuvering. The resulting controllers must provide for the integration of both conventional and unconventional control effectors.

Modern robust multivariable design methods provide an efficient means of developing linear controllers for aircraft. Because the flight control problem is inherently multivariable, and the linear aircraft model has associated uncertainties, robust multivariable methods are a good choice for flight control design when nonlinearities are not too severe. In a Flight Dynamics Directorate contracted effort,[2,3] a robust H_∞ controller within an inner/outer loop framework was designed for a supermaneuverable aircraft at a single flight condition, and robust performance was demonstrated for a Herbst-like maneuver. A robust controller for this same vehicle was designed by Sparks and Banda[4] for a single flight condition using μ synthesis in a model-following framework to simultaneously incorporate flying qualities specifications and account for structured uncertainty. A recent Wright Laboratory technical report[5] describes the design of a μ synthesis controller for a supermaneuverable vehicle that is integrated into an inner/outer loop control structure to provide full-envelope robust stability and performance for angles of attack up to 25 deg.

Traditionally, flight control law development for low- to moderate-angle-of-attack flight regimes has been accomplished using linear design methods on linearized models of the aircraft. However, the advantages of supermaneuverability dictate that future air combat will venture into high-angle-of-attack, nonlinear flight regions. Purely linear controllers are not able to effectively control supermaneuverable aircraft for more than very limited flight envelopes. This limitation has motivated a number of researchers to explore nonlinear techniques such as dynamic inversion. Bugajski and Enns[6] have used nonlinear dynamic inversion to control the High-Angle-of-Attack Research Vehicle (HARV) aircraft across a wide, high-angle-of-attack flight envelope. Snell et al.[7] compared the performance of a dynamic inversion control system to one designed using conventional gain scheduling. Huang et al.[8] have used a dynamic inversion approach to develop high-angle-of-attack control laws for the X-29.

High-angle-of-attack maneuvering is still a relatively new area in flight controls. Venturing into the regions of poststall flight can and should elicit serious questions about safety issues such as control effector saturation and departure susceptibility. Different methods have been successfully demonstrated that assist in preventing the destabilizing effects of control saturations. In an approach used by Bugajski and Enns,[6] loop bandwidths are reduced so that a scaled projection of the desired control vector is achieved and the control surfaces lie on the boundary of an achievable subspace. A method of allocating control effectors such that the maximum possible moment is generated within a constrained set of achievable values has been suggested by Durham.[9] Another approach introduces thrust vectoring controls when saturations occur in aerodynamic surfaces.[5]

The main contribution of the work presented in this paper is the integration of some of the most promising approaches described previously into a detailed design approach for achieving robust high-angle-of-attack flight control designs. The most notable advancement is the integration of dynamic inversion and structured singular value synthesis. Linearization of the vehicle dynamics is accomplished through a nonlinear dynamic inversion scheme. A robust compensator is designed around the linearized plant using μ synthesis in a model-following framework. The μ-synthesis design satisfies flying qualities requirements and robustness goals throughout the design envelope. A control allocation scheme is used which uses the pseudoinverse of the control distribution matrix to allocate controls based on body axis rotational acceleration commands. A method known as daisy chaining is used to generate thrust vectoring commands when aerodynamic control effector saturation occurs. Adverse control power saturation effects are minimized by scaling lateral commands based on an achievable control vector. Control effector prioritization is implemented through a daisy-chain technique that limits lateral control power demands that compete with longitudinal power requirements.

Received June 15, 1993; presented as Paper 93-3774 at the AIAA Guidance, Navigation, and Control Conference, Monterey, CA, Aug. 9–11, 1993; revision received Sept. 30, 1993; accepted for publication Oct. 1, 1993.

*Stability and Control Engineer, Wright Laboratory. Member AIAA.
†Aerospace Engineer, Wright Laboratory. Member AIAA.
‡Aerospace Engineer, Wright Laboratory. Associate Fellow AIAA.

In the following sections, a description of a modified F-18 aircraft model is given followed by the definition of design requirements. A brief theoretical background is presented on nonlinear dynamic inversion and μ synthesis. The controller architecture and design is described followed by the control allocation scheme and departure resistance logic. Finally, linear robustness analysis results and the results of a high-fidelity, nonlinear simulation of a supermaneuver are presented.

Aircraft Model

The aircraft model described in this paper is based upon a modified version of the F-18 aircraft. The vehicle is a twin-engine fighter aircraft with a moderately swept wing, twin canted vertical tails, and a large leading-edge root extension. The aircraft model is augmented with two-dimensional thrust vectoring nozzles that provide pitch and yaw moments when deflected symmetrically and a roll moment when deflected asymmetrically. The aerodynamic control inputs to the aircraft dynamics are the elevators, the ailerons, the rudders, and the leading- and trailing-edge flaps. The aerodynamic surfaces are useful at normal flight conditions, where there is adequate aerodynamic control surface effectiveness. The thrust vectoring inputs are useful at high-angle-of-attack, low-dynamic-pressure operating conditions, where the traditional aerodynamic control effectiveness is inadequate. The pilot inputs include a control stick and rudder pedals.

A nonlinear simulation model of this aircraft exists as a modular FORTRAN code. The model consists of separate modules describing the atmosphere, nonlinear equations of motion, aerodynamics, engines, thrust vectoring nozzles, variable geometry inlets, sensors, and actuators which include rate and position limits. The high-fidelity model was developed as part of a previous effort which gives more detail than that presented here.[10] There are five pairs of aerodynamic surfaces: three pairs for active control and two pairs scheduled for optimum performance. The ailerons, rudders, and elevators are used for stability augmentation and flight path manipulation. The leading- and trailing-edge flaps are scheduled to maximize airframe performance across the flight envelope. The aerodynamic data are contained in tabular format and linear interpolation is used for traditional force and moment aerodynamic coefficient buildup. Thrust vectoring-induced aerodynamic effects are added to static and dynamic baseline aerodynamic coefficients to obtain total aerodynamic coefficients.

The dynamics of this vehicle can be described by the following set of first-order nonlinear differential equations.[6,11] The first three equations describe the rotational dynamics of the aircraft in the body axis.

$$\dot{q} = (1/Iy)\ [m_{\text{aero}} + m_{\text{thrust}} + pr(I_z - I_x) + I_{xz}(r^2 - p^2)] \quad (1)$$

$$\begin{bmatrix} \dot{p} \\ \dot{r} \end{bmatrix} = \begin{bmatrix} I_x & -I_{xz} \\ -I_{xz} & I_z \end{bmatrix}^{-1} \times \begin{bmatrix} l_{\text{aero}} + l_{\text{thrust}} + pqI_{xz} + qr(I_y - I_z) \\ n_{\text{aero}} + n_{\text{thrust}} - qrI_{xz} + pq(I_x - I_y) \end{bmatrix} \quad (2)$$

Here, q, p, and r are the body axis pitch, roll, and yaw rates, respectively. I_x, I_y, I_z, and I_{xz} are the moments of inertia. The m, l, and n terms are the aerodynamic and thrust moment contributions to the rotational equations of motion.

The next three equations describe the evolution of aircraft motion with respect to its velocity vector.

$$\dot{\alpha} = q - (p \cos\alpha + r \sin\alpha)\tan\beta - \frac{\cos\mu}{\cos\beta}\dot{\gamma} - \sin\mu\frac{\cos\gamma}{\cos\beta}\dot{\chi} \quad (3)$$

$$\dot{\beta} = p \sin\alpha - r\cos\alpha - \sin\mu\dot{\gamma} + \cos\mu\cos\gamma\dot{\chi} \quad (4)$$

$$\dot{\mu} = \frac{\cos\alpha}{\cos\beta}p + \frac{\sin\alpha}{\cos\beta}r + \tan\beta\cos\mu\gamma + [\sin\gamma + \tan\beta\sin\mu\cos\gamma]\dot{\chi} \quad (5)$$

Here, α, β, and μ are the angle of attack, sideslip angle, and roll angle about the velocity vector.

The last three equations describe the orientation of the velocity vector with respect to inertial space.

$$\dot{\gamma} = \frac{\cos\mu}{mV}L - \frac{\cos\beta\sin\mu}{mV}Y - \frac{\cos\gamma}{V}g + \frac{1}{mV}F_{\text{thrust}_\gamma} \quad (6)$$

$$\dot{\chi} = \frac{1}{mV\cos\gamma}[\sin\mu L + \cos\beta\cos\mu Y] + \frac{1}{mV}F_{\text{thrust}_\chi} \quad (7)$$

$$\dot{V} = -\frac{D}{m} - g\sin\gamma + \sin\beta Y + \frac{1}{m}F_{\text{thrust}_V} \quad (8)$$

Here, γ is the flight path angle, χ is the ground track angle, and V is the velocity. The F_{thrust} terms are the linear contributions of vehicle thrust to the aircraft equations of motion, resolved into the respective vectors. L, D, and Y are lift, drag, and side force, respectively. The parameter m is vehicle mass, and g is gravitational acceleration.

Design Requirements

Flying qualities are the primary measures of performance for a manual flight control system. For conventional flight, specifications for flying qualities can be found in MIL-STD-1797A.[12] While these requirements are not valid for high-angle-of-attack flight, enough guidance is given to provide a basis for extrapolation. A rigorous study of new flying qualities measures is beyond the scope of this paper. The following high-α requirements are defined here only as baselines for this design study.

Requirements for the short period mode include constraints on the frequency and damping of a low-order fit of the transfer function between pilot inputs and aircraft pitch response. Appropriate forms for this low-order transfer function and methods for deriving the low-order fit are described in MIL-STD-1797A.[12] Short period frequency ω_{sp} should be a function of equivalent airspeed V_{eq}. An appropriate guideline for short period frequency is:

$$\omega_{sp}(\text{rad/s}) \approx 1.0 \times (V_{eq}\ (\text{ft/s})/100) \quad (9)$$

Therefore, the desired pitch response speed to pilot commands should increase with equivalent airspeed. At flight conditions above a 30-deg angle of attack, short period damping should be at the high end of the military standard's level 1 and 2 requirements. For these conditions, the acceptable range for ζ_{sp} is between 0.7–2.0.

The primary roll subsidence mode flying quality parameter is roll mode time constant, T_R. The roll mode time constant is found from a first-order fit of the transfer function between pilot input and roll rate response. Past experience with fighter aircraft has shown that desired values for T_R are a function of angle of attack. MIL-STD-1797A level 2 requirements are used as a baseline range of acceptable roll mode time constants. The target values used in this study are: $T_R = 0.30$ at $\alpha = 0$ deg, $T_R = 0.75$ at $\alpha = 30$ deg, and $T_R = 1.40$ at $\alpha = 60$ deg.

The desired directional response to pilot inputs can be derived from requirements on the Dutch roll mode. Dutch roll frequency, ω_D, and damping, ζ_D, can be derived from a second-order fit of the transfer function between pilot input and sideslip response. Because of the danger of departure susceptibility at high angles of attack, the Dutch roll damping is required to be greater than 0.8. The Dutch roll frequency requirement is taken directly form MIL-STD-1797A, $\omega_D \geq 1.0$ rad/s.

Dynamic Inversion

The purpose of dynamic inversion is to develop a feedback control law that linearizes the plant response to commands. In general the nonlinear aircraft dynamics can take the form

$$\dot{x} = f(x, u), \qquad y = Cx \tag{10}$$

where x is an n-dimensional state vector, u is an m-dimensional input vector, C is a $p \times n$ matrix, and y is a p-dimensional vector of output variables. A transformation is necessary to put the equations in a form from which the inverse dynamics can be constructed. Each controlled output, y_i, is differentiated until an input term from u appears.[13] Only m outputs can be controlled independently by the m available inputs, therefore p must equal m. As shown by Lane and Stengel,[14] the output equations may now be written in the form

$$y^{[d]} = \begin{bmatrix} y_1^{[d_1]} \\ y_2^{[d_2]} \\ \vdots \\ y_p^{[d_p]} \end{bmatrix} = h(x) + G(x)u \tag{11}$$

where $y_i^{[d_i]}$ represents the d_ith derivative of the output y_i. The inverse dynamics control law can be written as

$$u = G(x)^{-1}[\nu - h(x)] \tag{12}$$

$h(x)$ represents the nonlinear output dynamics and $G(x)$ represents the nonlinear control distribution. The parameter ν represents the desired linear dynamics of the closed-loop system. With the inverse dynamics control law implemented, the closed-loop system now has the form

$$y^{[d]} = \nu \tag{13}$$

If the system is observable and $\Sigma_{i=1}^{p} d_i = n$, then all of the closed-loop poles may be placed. If $\Sigma_{i=1}^{p} d_i < n$, then closed-loop stability cannot be proven. In this case the unobserved dynamics or the internal dynamics of dynamic inversion must be checked at local operating points to insure stability.[14]

Structured Singular Value Synthesis

The structured singular value (μ) framework provides a unifying measure which can be used to simultaneously address stability and performance robustness specifications.[15,16] If μ is less than unity for a properly scaled system, then the specifications are met. It is desirable to be able to address these multiple objectives directly within a design method. μ synthesis provides for the direct incorporation of robust stability and performance goals into a design by combining H_∞ design with structured singular value analysis.[17,18] The μ-synthesis problem is described by the attempt to find a controller that minimizes an upper bound on the structured singular value,

$$\min_{K} \inf_{D \in D} \sup_{\omega} \bar{\sigma}[DM(K)D^{-1}] \tag{14}$$

where $M(K)$ is the weighted closed-loop transfer function.

One approach to this problem is the DK iteration; it calls for alternately minimizing sup $\bar{\sigma}[DM(K)D^{-1}]$ for either K or D while holding the other constant. First the controller synthesis problem is solved using H_∞ design on the nominal design model. μ analysis is then performed on the closed-loop transfer function $M(K)$, producing values of the D scaling matrices at each frequency. The resulting frequency response data are fit with an invertible, stable, minimum phase transfer function which becomes part of the nominal synthesis structure. With D fixed, the controller synthesis problem is again solved by performing an H_∞ design on the augmented system. The DK iterations are continued until a satisfactory controller is found or a minimum is reached. The resulting controller order is the order of the design plant and weighting matrices, in addition to the order of the D-scale transfer function fits. With each iteration, the D-scale frequency response data from the previous iteration is combined with the current values, and then the transfer function fit is performed on the combined data. This approach avoids a built-in increase in controller order that would result if at each iteration new D-scale fit transfer functions were augmented into the synthesis model from the previous step. It is important to note that the DK iteration is not guaranteed to converge to a global minimum, but practical experience has shown that the method works well for a broad class of problems.[18]

Control Law Development

Dynamic inversion and structured singular value synthesis are combined to achieve robust manual control for high-angle-of-attack flight. The controller structure is shown in Fig. 1. Pilot pitch stick inputs command a pitch rate q_{ref}, roll stick inputs command a stability axis roll rate $\dot{\mu}_{\text{ref}}$, and pedal inputs command a sideslip β_{ref}. The following sections describe each element of the control design.

Fast Inversion

The aerodynamic and thrust induced moments in Eqs. (1) and (2) determine the classical linear stability and control characteristics of the aircraft. These terms may be expanded into derivative form.

$$m_{\text{aero}} = [C_{m\alpha}V\alpha + (\bar{c}/2)\, C_{mq}q + C_{m_{\delta_E}}V\delta_E]\, \tfrac{1}{2}\, \rho VS\bar{c} \tag{15}$$

$$l_{\text{aero}} = [C_{l\beta}V\beta + (\bar{b}/2)\, C_{lp}p + (\bar{b}/2)\, C_{lr}r + C_{l_{\delta_{DT}}}V\delta_{DT} + C_{l_{\delta_A}}V\delta_A + C_{l_{\delta_R}}V\delta_R]\, \tfrac{1}{2}\, \rho VS\bar{b} \tag{16}$$

$$n_{\text{aero}} = [C_{n\beta}V\beta + (\bar{b}/2\, C_{np}p + (\bar{b}/2)\, C_{nr}r + C_{n_{\delta_{DT}}}V\delta_{DT} + C_{n_{\delta_A}}V\delta A + C_{n_{\delta_R}}V\delta_R]\, \tfrac{1}{2}\, \rho VS\bar{b} \tag{17}$$

$$m_{\text{thrust}} = [C_{m_{\delta_{\text{PTV}}}}V\delta_{\text{PTV}}]\, \tfrac{1}{2}\, \rho VS\bar{c} \tag{18}$$

$$l_{\text{thrust}} = [C_{l_{\delta_{\text{RTV}}}}V\delta_{\text{RTV}} + C_{l_{\delta_{\text{YTV}}}}V\delta_{\text{YTV}}]\, \tfrac{1}{2}\, \rho VS\bar{b} \tag{19}$$

$$n_{\text{thrust}} = [C_{n_{\delta_{\text{RTV}}}}V\delta_{\text{RTV}} + C_{n_{\delta_{\text{YTV}}}}V\delta_{\text{YTV}}]\, \tfrac{1}{2}\, \rho VS\bar{b} \tag{20}$$

where S is the wing area, $\bar{c}$ is the mean aerodynamic chord, and $\bar{b}$ is the wing span. δ_E is the symmetric elevator position, δ_{DT} is the asymmetric elevator position, δ_A is the aileron position, δ_R is the rudder position, δ_{PTV} is the symmetric pitch thrust vectoring nozzle position, δ_{RTV} is the asymmetric pitch (roll) thrust vectoring nozzle position, and δ_{YTV} is the yaw thrust vectoring nozzle position. The derivatives in Eqs. (15–20) can be represented in dimensional form where:

$$M_q = \frac{\rho VS\bar{c}^2}{4I_y} C_{m_q}, \qquad M_{\alpha,\delta} = \frac{\rho V^2 S\bar{c}}{2I_y} C_{m_{\alpha,\delta}} \tag{21}$$

$$L^*_{p,r} = \frac{\rho VS\bar{b}^2}{4I_X} C_{l_{p,r}}, \qquad L^*_{\beta,\delta} = \frac{\rho V^2 S\bar{b}}{2I_X} C_{l_{\beta,\delta}} \tag{22}$$

$$N^*_{p,r} = \frac{\rho VS\bar{b}^2}{4I_Z} C_{N_{p,r}}, \qquad N^*_{\beta,\delta} = \frac{\rho V^2 S\bar{b}}{2I_Z} C_{n_{\beta,\delta}} \tag{23}$$

$$L_{\beta,p,r,\delta} = \left(L^*_{\beta,p,r,\delta} + \frac{I_{XZ}}{I_X} N^*_{\beta,p,r,\delta}\right) \frac{I_Z I_X}{(I_Z I_X - I^2_{XZ})} \tag{24}$$

$$N_{\beta,p,r,\delta} = \left(N^*_{\beta,p,r,\delta} + \frac{I_{XZ}}{I_Z} L^*_{\beta,p,r,\delta}\right) \frac{I_Z I_X}{(I_Z I_X - I^2_{XZ})} \tag{25}$$

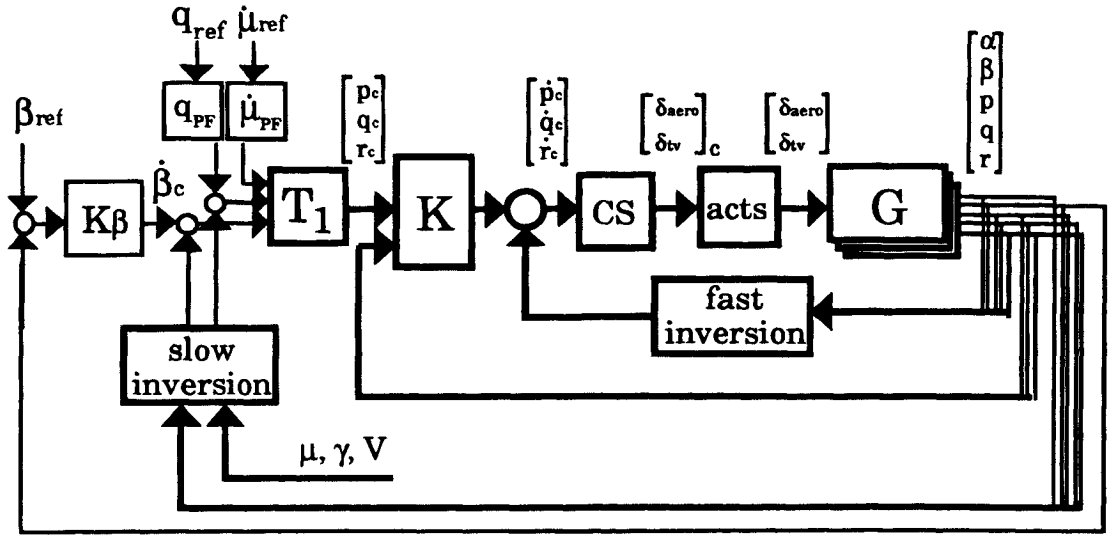

Fig. 1 Closed-loop system.

$$Z_{\alpha,\delta} = (\rho V^2 S/2m)\, C_{z\alpha,\delta} \tag{26}$$

$$Y_{\beta,\delta} = (\rho V^2 S/2m)\, C_{y\beta,\delta} \tag{27}$$

The rotational equations of motion can now be written as a combination of linear and nonlinear contributions.

$$\begin{bmatrix}\dot{p}\\ \dot{q}\\ \dot{r}\end{bmatrix} = \begin{bmatrix}0 & L_\beta & L_p & 0 & L_r\\ M_\alpha & 0 & 0 & M_q & 0\\ 0 & N_\beta & N_p & 0 & N_r\end{bmatrix}\begin{bmatrix}\alpha\\ \beta\\ p\\ q\\ r\end{bmatrix} + \begin{bmatrix}I_X & 0 & -I_{XZ}\\ 0 & I_y & 0\\ -I_{XZ} & 0 & I_Z\end{bmatrix}^{-1}\begin{bmatrix}pqI_{XZ} + qr(I_y - I_Z)\\ pr(I_Z - I_X) + I_{XZ}(r^2 - p^2)\\ -qrI_{XZ} + pq(I_X - I_y)\end{bmatrix} + \begin{bmatrix}0 & L_{\delta_{DT}} & L_{\delta_A} & L_{\delta_R}\\ M_{\delta_E} & 0 & 0 & 0\\ 0 & N_{\delta_{DT}} & N_{\delta_A} & N_{\delta_R}\end{bmatrix}\begin{bmatrix}\delta_E\\ \delta_{DT}\\ \delta_A\\ \delta_R\end{bmatrix} + \begin{bmatrix}0 & L_{\delta_{RTV}} & L_{\delta_{YTV}}\\ M_{\delta_{PTV}} & 0 & 0\\ 0 & N_{\delta_{RTV}} & N_{\delta_{YTV}}\end{bmatrix}\begin{bmatrix}\delta_{PTV}\\ \delta_{RTV}\\ \delta_{YTV}\end{bmatrix} \tag{28}$$

At this point, it is assumed that a generalized control scheme has been implemented in the form of a control selector, described later in this paper. Equation (28) can be rewritten in terms of the generalized controls: roll, pitch, and yaw acceleration commands.

$$\begin{bmatrix}\dot{p}\\ \dot{q}\\ \dot{r}\end{bmatrix} = \begin{bmatrix}0 & L_\beta & L_p & 0 & L_r\\ M_\alpha & 0 & 0 & M_q & 0\\ 0 & N_\beta & N_p & 0 & N_r\end{bmatrix}\begin{bmatrix}\alpha\\ \beta\\ p\\ q\\ r\end{bmatrix} + \begin{bmatrix}I_X & 0 & -I_{XZ}\\ 0 & I_y & 0\\ -I_{XZ} & 0 & I_Z\end{bmatrix}^{-1}\begin{bmatrix}pqI_{XZ} + qr(I_y - I_Z)\\ pr(I_Z - I_X) + I_{XZ}(r^2 - p^2)\\ -qrI_{XZ} + pq(I_X - I_y)\end{bmatrix} + \begin{bmatrix}1 & 0 & 0\\ 0 & 1 & 0\\ 0 & 0 & 1\end{bmatrix}\begin{bmatrix}\dot{p}_c\\ \dot{q}_c\\ \dot{r}_c\end{bmatrix} \tag{29}$$

The first step in control law development is the implementation of a dynamic inversion loop that replaces the existing rotational aircraft dynamics with some set of desired dynamics. This step is called the fast inversion.

$$\begin{bmatrix}\dot{p}_c\\ \dot{q}_c\\ \dot{r}_c\end{bmatrix} = \begin{bmatrix}\dot{p}_{des}\\ \dot{q}_{des}\\ \dot{r}_{des}\end{bmatrix} - \begin{bmatrix}0 & L_\beta & L_p & 0 & L_r\\ M_\alpha & 0 & 0 & M_q & 0\\ 0 & N_\beta & N_p & 0 & N_r\end{bmatrix}\begin{bmatrix}\alpha\\ \beta\\ p\\ q\\ r\end{bmatrix} - \begin{bmatrix}I_X & 0 & -I_{XZ}\\ 0 & I_y & 0\\ -I_{XZ} & 0 & I_z\end{bmatrix}^{-1}\begin{bmatrix}pqI_{XZ} + qr(I_y - I_Z)\\ pr(I_Z - I_X) + I_{XZ}(r_z^2 - p^2)\\ -qrI_{XZ} + pq(I_X - I_y)\end{bmatrix} \tag{30}$$

Equation (30) is the application of the dynamic inversion step in Eq. (12) to the outputs p, q, and r. The stability derivatives and inertial properties in Eq. (30) are found through linear interpolation of values stored in a tabular database. The desired dynamics contain a set of linear stability derivatives that provide satisfactory modal frequency and damping characteristics.

$$\begin{bmatrix}\dot{p}_{des}\\ \dot{q}_{des}\\ \dot{r}_{des}\end{bmatrix} = \begin{bmatrix}0 & L'_\beta & L'_p & 0 & L'_r\\ M'_\alpha & 0 & 0 & M'_q & 0\\ 0 & N'_\beta & N'_p & 0 & N'_r\end{bmatrix}\begin{bmatrix}\alpha\\ \beta\\ p\\ q\\ r\end{bmatrix} + \begin{bmatrix}1 & 0 & 0\\ 0 & 1 & 0\\ 0 & 0 & 1\end{bmatrix}\begin{bmatrix}\dot{p}'_c\\ \dot{q}'_c\\ \dot{r}'_c\end{bmatrix} \tag{31}$$

Structured Singular Value Synthesis

The fast inversion control law provides equalization of the dominant dynamics across the flight envelope. This equalization effectively eliminates the requirement for gain scheduling. A robust controller may now be designed around the linearizing fast inversion loop to provide command tracking performance. Robust tracking of body axis rotational rate commands is achieved with a μ-synthesis controller. The structured singular value of two uncertainty and one performance block is minimized using a DK iteration. As shown in Fig. 2, three frequency-dependent weights are chosen to balance performance and robustness considerations.

The design plant is defined by $G^* = C^*(sI - A^*)^{-1} B^* \cdot A^*$ is the system dynamics matrix at some flight condition which is considered to be central to the flight envelope in terms of modal frequencies and damping. B^* is the normalized con-

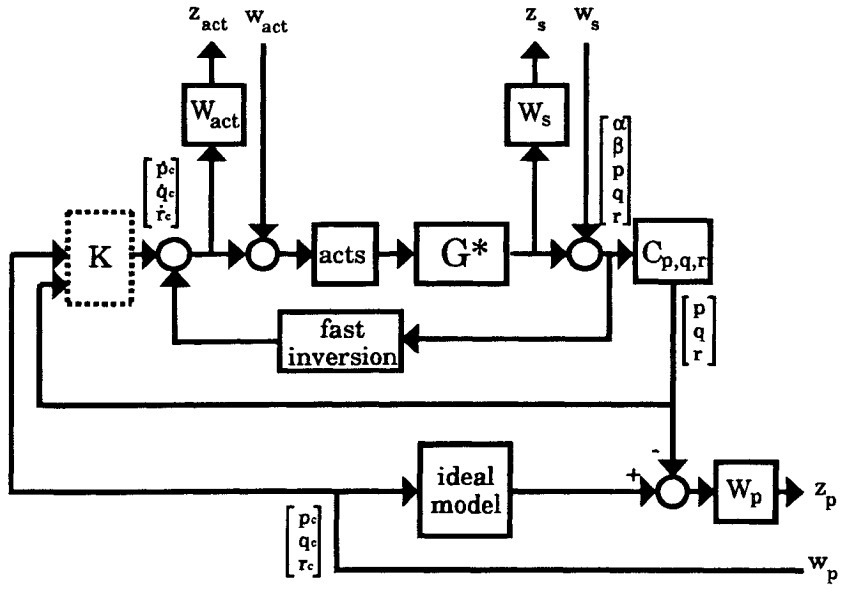

Fig. 2 Design model for μ synthesis.

trol effectiveness matrix in Eq. (29). C^* produces the outputs α, β, p, q, and r. The fast inversion block represents the body axis rate inversions shown in Eq. (30).

W_{act} defines the uncertainty at the actuator input, W_s defines the uncertainty at the sensor output, and W_p weights the error between the complementary sensitivity function of the closed-loop system and an ideal model of the system response. The actuator and sensor uncertainty models are taken from Haiges, et al.[19] W_p is chosen such that the closed-loop system follows the ideal model closely at frequencies below 10 rad/s. The ideal model represents the desired transfer function between body axis rate commands and roll, pitch, and yaw rate responses. For this problem it is defined as

$$\text{Ideal Model} = \begin{bmatrix} \frac{p}{p_c} & \frac{q}{q_c} & \frac{r}{r_c} \end{bmatrix} I_{3\times 3} = \begin{bmatrix} \frac{3}{s+3} & \frac{3}{s+3} & \frac{3}{s+3} \end{bmatrix} I_{3\times 3} \tag{32}$$

A successful μ-synthesis design achieves this first-order tracking response to body axis rotational rate commands. The diagonal structure of the ideal model forces the response to be decoupled in roll, pitch, and yaw. The resulting compensator is 42nd order. Using balanced truncation, the order is reduced to 19 without any loss of closed-loop performance or robustness.

Slow Inversion

Because only three generalized controls are available, the first step in dynamic inversion ignores the dynamics associated with angle of attack and sideslip. These internal dynamics can be accounted for in a second application of dynamic inversion to these slower state dynamics. A simple unitary transformation can be made to translate stability axis rate commands into the body axis rate commands that are available to the μ-synthesis controller.

$$\begin{bmatrix} p_c \\ q_c \\ r_c \end{bmatrix} = T_1 \begin{bmatrix} \dot{\mu}_c \\ \dot{\alpha}_c \\ \dot{\beta}_c \end{bmatrix}, \qquad T_1 = \begin{bmatrix} \cos\alpha & 0 & \sin\alpha \\ 0 & 1 & 0 \\ \sin\alpha & 0 & -\cos\alpha \end{bmatrix} \tag{33}$$

Notice that q_c is equal to $\dot{\alpha}_c$. Equations (3) and (4) can be rewritten by replacing the rotational rates with these commands. F_{thrust_y} and F_{thrust_x} are assumed to be negligible.

$$\dot{\alpha} = q_c - (p\cos\alpha + r\sin\alpha)\tan\beta + \frac{\cos\mu\cos\gamma}{V\cos\beta}g - \frac{L}{mV\cos\beta} \tag{34}$$

$$\dot{\beta} = \dot{\beta}_c + \sin\mu\cos\gamma\frac{g}{V} + \frac{Y\cos\beta}{mV} \tag{35}$$

If sufficient frequency separation exists between the body axis rate command responses and a contribution to the $\dot{\alpha}$ and $\dot{\beta}$ equations, then that contribution can be canceled by a slow inversion loop. The inversion control law for q_c includes the change in lift with angle of attack and the nonlinear effect of gravitational acceleration due to vehicle orientation. The roll and yaw rate terms in the $\dot{\alpha}$ equation are considered to be too fast to be controlled.

$$q_c = q_c' - \frac{\cos\mu\cos\gamma}{V\cos\beta}g - \frac{Z_\alpha}{mV\cos\beta} \tag{36}$$

The inversion control law for the sideslip rate equation includes sideforce contribution of the sideslip angle and the nonlinear term representing gravity induced sideslip rate due to nonzero roll angle.

$$\dot{\beta}_c = -\sin\mu\cos\gamma\frac{g}{V} + \left(K_\beta + \frac{Y_\beta\cos\beta}{mV}\right)(\beta_{\text{ref}} - \beta) \tag{37}$$

The additional sideslip feedback term in this equation provides sideslip command tracking and increased turn coordination. The gain K_β is selected to provide a sideslip response that satisfies the frequency and damping requirements for the Dutch roll mode.

Command Shaping

The desired flying qualities for the pitch and roll axis are achieved through the use of prefilters. By scheduling these prefilters, the response to pilot inputs can be shaped appropriately with flight condition. As described earlier, the desired roll response is first order with a time constant that is a function of angle of attack. With the μ-synthesis compensator implemented, we can assume that the stability axis roll rate transfer function is:

$$\frac{\dot{\mu}}{\dot{\mu}_c} \approx \frac{3}{(s+3)} \tag{38}$$

so the response with a first-order prefilter with gain K_μ is:

$$\frac{\dot{\mu}}{\dot{\mu}_{ref}} = [\dot{\mu}_{PF}]\frac{\dot{\mu}}{\dot{\mu}_c} \approx \frac{3K_\mu}{(s+3)(s+K_\mu)} \approx \frac{3K_\mu}{[s^2+(3+K_\mu)s+3K_\mu]} \tag{39}$$

A schedule for the roll prefilter gain that achieves the desired equivalent system response with angle of attack is:

$$K_\mu = 3.65 - 0.0433\,\alpha \quad \text{and} \quad \min(K_\mu) = 0.5 \tag{40}$$

The desired pitch response to pilot inputs is second order with a short period frequency that is a function of equivalent airspeed. The transfer function representing the pitch response to pilot commands is:

$$\frac{q}{q_c'} \approx \frac{3}{(s+3)} \tag{41}$$

The pitch response with a first-order prefilter with gain K_q is:

$$\frac{q}{q_{ref}} = [q_{PF}]\frac{q}{q_c'} \approx \frac{3K_q}{(s+3)(s+K_q)} \approx \frac{3K_q}{[s^2+(3+K_q)s+3K_q]} \tag{42}$$

The prefilter gain K_q is scheduled to provide the desired level of damping and increase in short period frequency with equivalent airspeed.

$$K_q = \frac{1}{3}\left(\frac{V_{eq}(kt)}{100}\right)^2 \tag{43}$$

Control Limiting and Prioritization

The control selector, sometimes referred to as pseudocontrols, has two functions. The first is to normalize control effectiveness by transforming generalized rotational rate commands into actuator position commands. The second is to take advantage of available control redundancy by allowing for control redistribution without changing the linear closed-loop performance. The basic idea of the control selector is in redefining the control contribution to the state equation (28) and (29),

$$B\delta = B^*\delta^* \tag{44}$$

B and δ are the actual control effectiveness matrix and control vector, and B^* and δ^* are the generalized control effectiveness

Table 1 Flight conditions for linear analysis

Flight condition	Mach	Altitude, ft	Angle-of-attack, deg	Equivalent airspeed, ft/s
1	0.2	10,000	30	109.7
2	0.2	10,000	45	109.7
3	0.2	10,000	60	109.7
4	0.2	30,000	75	72.09
5	0.4	30,000	50	144.2
6	0.6	30,000	20	216.3
7	0.6	30,000	30	216.3

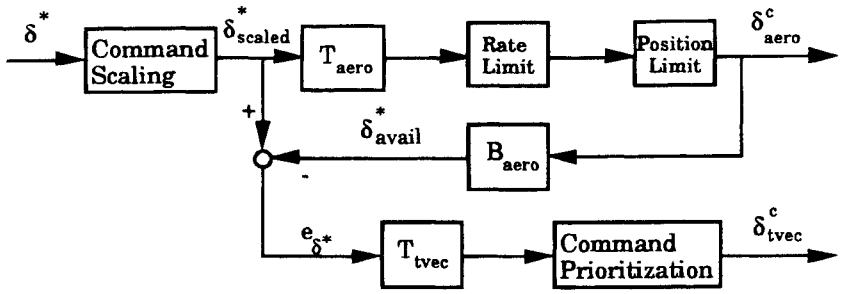

Fig. 3 Nonlinear control selector.

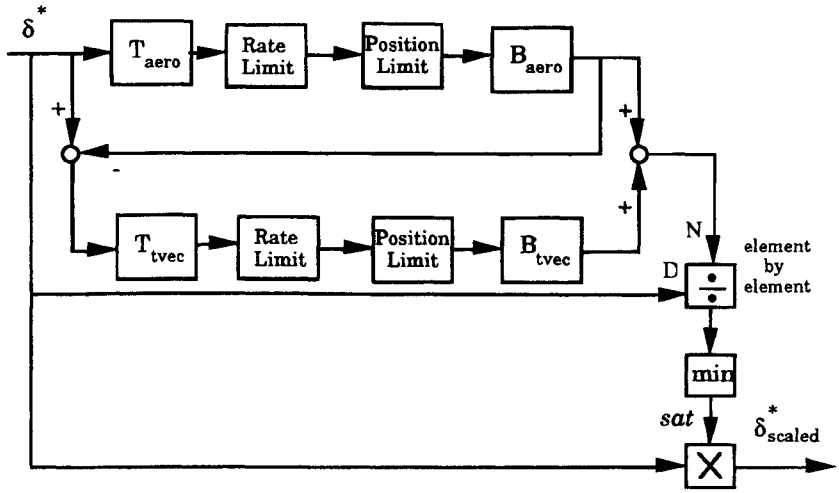

Fig. 4 Command scaling logic.

matrix and control vector. The actual control can now be defined in terms of the generalized control,

$$\delta = T\delta^* \tag{45}$$

The transformation T is the control selector. It is defined simply by

$$T = N(BN)^{\#}B^* \tag{46}$$

The operation ( ) is a pseudoinverse and N is a matrix that may be used to combine controls or emphasize/de-emphasize a control channel in the case of redundant effectors. Because the B matrix in Eq. (46) is a function of flight condition and aircraft state, the control selector is a function of parameters such as Mach number, altitude, angle of attack, and engine power level angle.

The generalized and actual controls for the supermaneuverable vehicle are given by

$$\delta^* = [\dot{p}_c \ \dot{q}_c \ \dot{r}_c]^T, \quad \delta = [\delta_E \ \delta_{DT} \ \delta_A \ \delta_R \ \delta_{PTV} \ \delta_{RTV} \ \delta_{YTV}]^T \tag{47}$$

Consider the following partitioning of the control effector vector as shown in Eq. (28):

$$\delta = \begin{bmatrix} \delta_{aero} \\ \delta_{tvec} \end{bmatrix} \tag{48}$$

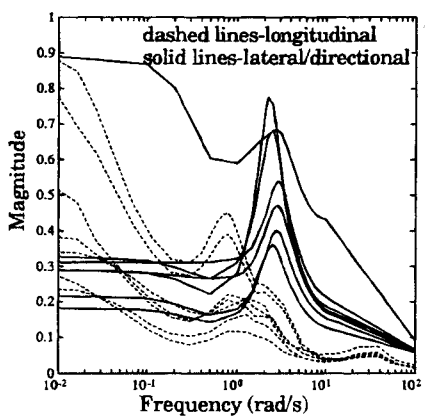

Fig. 5 Upper bounds on structured singular value.

where

$$\delta_{aero} = \begin{bmatrix} \delta_E \\ \delta_{DT} \\ \delta_A \\ \delta_R \end{bmatrix}, \qquad \delta_{tvec} = \begin{bmatrix} \delta_{PTV} \\ \delta_{RTV} \\ \delta_{YTV} \end{bmatrix}$$

resulting in

$$B_{aero} = \begin{bmatrix} 0 & L_{\delta_{DT}} & L_{\delta_A} & L_{\delta_R} \\ M_{\delta_E} & 0 & 0 & 0 \\ 0 & N_{\delta_{DT}} & N_{\delta_A} & N_{\delta_R} \end{bmatrix}$$

$$B_{tvec} = \begin{bmatrix} 0 & L_{\delta_{RTV}} & L_{\delta_{YTV}} \\ M_{\delta_{PTV}} & 0 & 0 \\ 0 & N_{\delta_{RTV}} & N_{\delta_{YTV}} \end{bmatrix} \tag{49}$$

With the preceeding partitions, Eq. (44) is written as:

$$[B_{aero}\, B_{tvec}] \begin{bmatrix} \delta_{aero} \\ \delta_{tvec} \end{bmatrix} = B^*\delta^* \tag{50}$$

here

$$B^* = \begin{bmatrix} 1 & 0 & 0 \\ 0 & 1 & 0 \\ 0 & 0 & 1 \end{bmatrix}$$

A daisy-chain method is used to generate thrust vector commands. Thrust vectoring is used only when the aerodynamic surfaces are not able to generate the necessary forces and moments required for commanded maneuvers. Therefore, the computation of aerodynamic control commands is independent of thrust vectoring control commands. The control selector is defined by

$$\delta_{aero} = T_{aero}\delta^* \qquad \delta_{tvec} = T_{tvec}\delta^* \tag{51}$$

and

$$T_{aero} = N_{aero}(B_{aero}N_{aero})^{\#} \qquad T_{tvec} = N_{tvec}(B_{tvec}N_{tvec})^{\#} \tag{52}$$

where N_{aero} and N_{tvec} are used to weight the redundant control effectors. Since the ailerons contribute more to the roll acceleration and the first priority of the horizontal tail should be pitch control, the differential horizontal tail command is reduced by weighting the command to be a quarter of the other aerodynamic

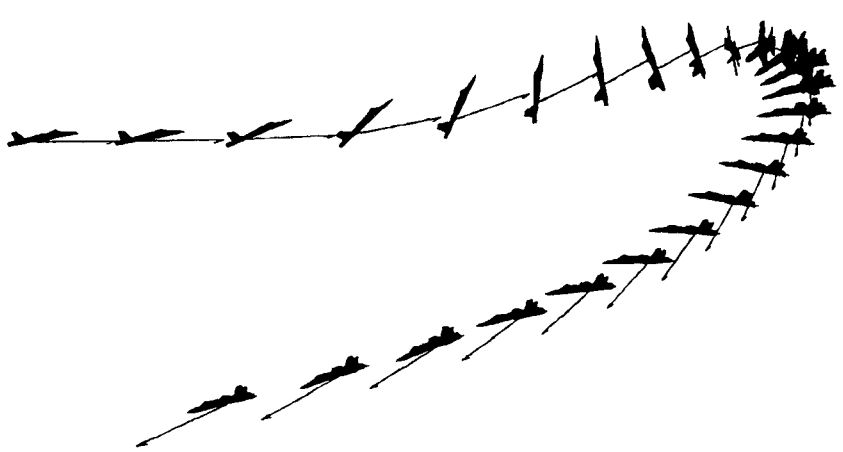

Fig. 6 High-angle-of-attack supermaneuver.

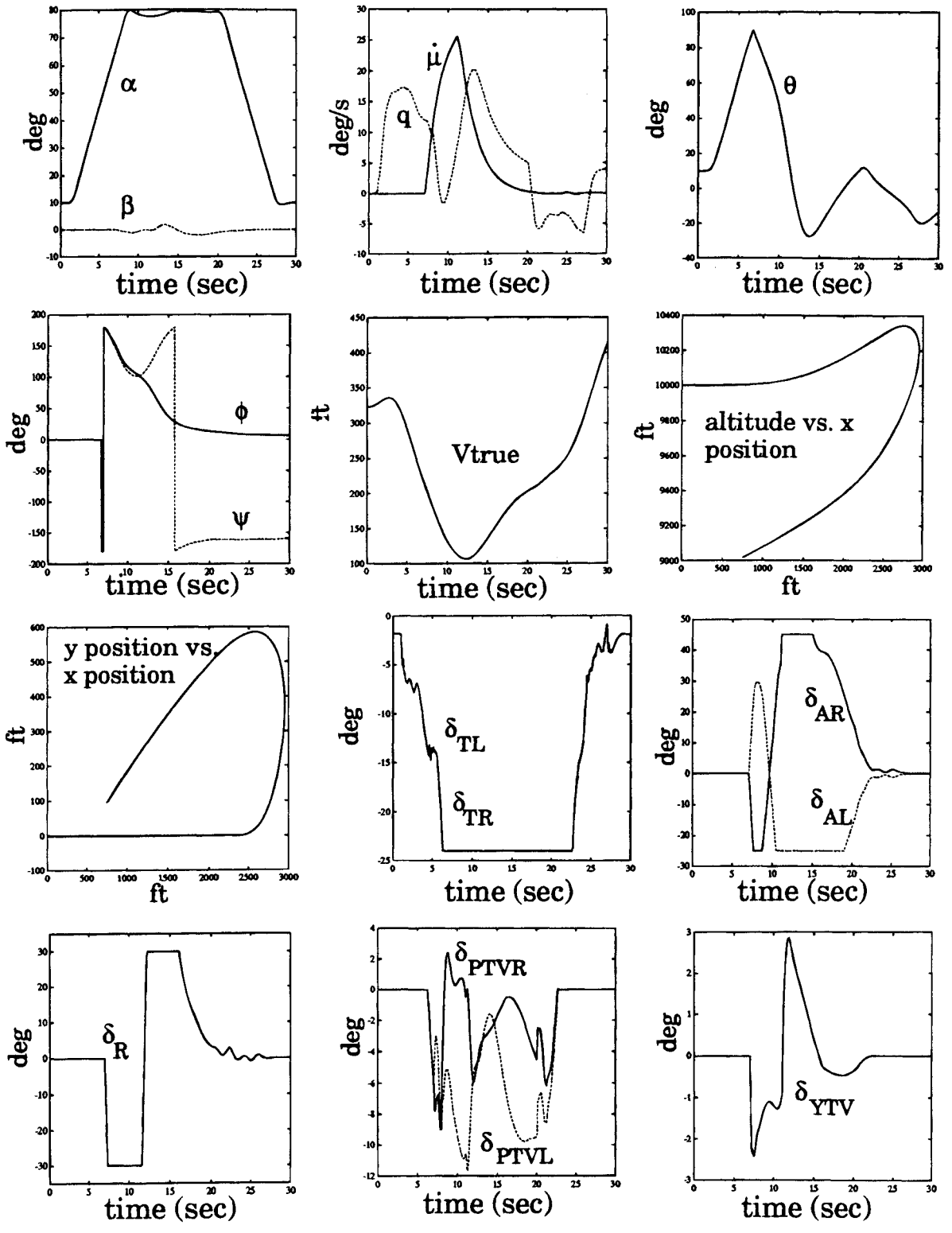

Fig. 7 Nonlinear time responses.

commands. There is no redundancy for the thrust vectoring control effectors, and thus, the weighting matrices become

$$N_{\text{aero}} = \begin{bmatrix} 1 & 0 & 0 & 0 \\ 0 & .25 & 0 & 0 \\ 0 & 0 & 1 & 0 \\ 0 & 0 & 0 & 1 \end{bmatrix} \qquad N_{\text{tvec}} = \begin{bmatrix} 1 & 0 & 0 \\ 0 & 1 & 0 \\ 0 & 0 & 1 \end{bmatrix} \tag{53}$$

Computation of the control selector, Eq. (51), depends on flight condition. Therefore, the elements of B_{aero} and B_{tvec} are found using linear interpolation of stored table values.

Nonlinear elements, such as position and rate limits, are required to implement the daisy-chain. Figure 3 shows the structure of the nonlinear control selector. A limited aerodynamic surface command (δ^{c}_{aero}) is generated from a rotational acceleration command (δ^{*}) via the aerodynamic control selector (T_{aero}), the aerodynamic surface limits, and command scaling logic. An achievable aerodynamic rotational acceleration vector ($\delta^{*}_{\text{avail}}$) is computed from the limited aerodynamic surface com-

mand using the control distribution (B_{aero}). The difference of the commanded and achievable rotational acceleration vectors ($e_{\delta *}$) is transformed to a thrust vector command (δ^{c}_{tvec}) using the thrust vector control selector (T_{tvec}) and command prioritization logic.

The command scaling logic limits the acceleration command in the event of control effector saturation. The lateral/directional generalized control command that is generated by the control system can be thought of as a vector. When saturation occurs in one axis, the resulting control vector loses both the magnitude and the direction of the desired control. By scaling the command vector in both axes, an achievable control vector can be realized that preserves the direction of the desired command and holds the limiting controls on their limits. A block diagram of the command scaling logic is shown in Fig. 4. The figure shows that the scaled vector is the product of the commanded vector and the minimum ratio of available and commanded acceleration, $\delta^{*}_{scaled} = \delta^{*} \times sat$. The scaling parameter, *sat*, is always less than or equal to unity. It can be argued that when saturations occur, control bandwidth is too high. An interpretation can be made that this scaling logic acts to reduce the control bandwidth in the event of control power saturation.[6]

The command prioritization logic limits the amount of commanded differential pitch (roll) thrust vectoring. By using models of rate and position limiters within a daisy chain, roll thrust vectoring is commanded only when the thrust vectoring nozzles are not saturated due to symmetric pitch thrust vectoring commands. For commanded rolls at high angles of attack, it can be interpreted that roll commands correspond to performance and pitch commands correspond to stability. Therefore, the pitch thrust vectoring command, and thus stability, has top priority.

Robustness Analysis

A range of flight conditions must be selected for the purpose of linear analysis. Table 1 describes the seven conditions that span a broad range of Mach numbers, altitudes, and angles of attack. Linearized models of the vehicle dynamics at these points are used for robustness analysis. The linear analysis models at each of these test conditions include high-order actuator models, vehicle dynamics, and control elements shown in Fig. 1.

The robustness of the closed-loop system is tested to simultaneous structured and unstructured uncertainties. The structured uncertainties consist of 19 real valued perturbations in the aerodynamic stability and control derivatives. The unstructured uncertainties include four frequency weighted complex perturbations in the actuator dynamics and five frequency weighted complex perturbations in the sensor dynamics. The resulting interconnection structure has 19 real 1×1 Δ blocks and nine complex 1×1 Δ blocks. More detailed information on the levels of uncertainty considered can be found in Buffington et al.[20] The quantities were derived as part of the work presented by Haiges et al.[19]

The results of structured singular value analysis indicate that the closed-loop system is robust to the levels of uncertainty considered. Figure 5 shows the upper bounds for the structured singular values at each of the linear test points. The fact that these bounds are less than unity at all frequencies provides a sufficient condition for robust stability. The peak in the lateral/directional bounds at 2–3 rad/s indicates that the Dutch roll mode is the most sensitive to plant uncertainties.

Nonlinear Results

To test the nonlinear performance of the flight control system, batch simulations are run on a high-fidelity, six-degree-of-freedom simulation of the supermaneuverable vehicle. A challenging supermaneuver that tests the performance of the control laws and the control distribution logic is a very high-angle-of-attack velocity vector roll. Figure 6 shows such a maneuver where the aircraft is pitched up to an 80-deg angle of attack and then rolled 180 deg about the velocity vector. This supermaneuver creates a rapid 180-deg change in heading angle. The solid arrows represent the aircraft's velocity vector. Figure 7 shows the time histories for this maneuver. Actuator positions are given in terms of left and right tail (δ_{TL}, δ_{TR}), left and right aileron (δ_{AL}, δ_{AR}), rudder (δ_R), left and right pitch thrust vectoring (δ_{PTVL}, δ_{PTVR}), and yaw thrust vectoring (δ_{YTV}). The left and right convention is used in place of symmetric and asymmetric so that control effector saturations are properly represented.

The 180-deg change in roll and heading angle is achieved by holding a 30-deg/s stability axis roll rate command for six seconds. The performance of the dynamic inversion/μ-synthesis control system is demonstrated by the smooth, well-damped stability axis roll rate response and the excellent turn coordination at an 80-deg angle of attack. Less than 2 deg of sideslip is generated during the supermaneuver. Notice that all of the aerodynamic surfaces saturate during this maneuver, forcing the control distribution, scaling, and prioritization logic to be activated. Command scaling comes into effect due to rate saturations in yaw thrust vectoring at the application and removal of the stability axis roll rate command. The pitch thrust vectoring prioritization logic is activated when symmetrical horizontal tail saturates, causing a requirement for symmetrical pitch thrust vectoring.

Conclusions

High-angle-of-attack control laws have been developed for a supermaneuverable vehicle with thrust vectoring capability. The methods of dynamic inversion and structured singular value synthesis are successfully integrated into a design approach which achieves desired performance and robustness levels. An advanced generalized controls approach is demonstrated for the allocation of redundant aerodynamic and thrust vectoring effectors. Command scaling and prioritization are implemented to minimize the destabilizing effects of saturations during demanding supermaneuvers. The design goals are achieved across a broad range of airspeeds, altitudes, and angles of attack. High-fidelity simulations show that the nonlinear aspects of the control laws perform well in a highly dynamic, nonlinear environment.

References

[1] Gal-Or, B., *Vectored Propulsion, Supermaneuverability and Robot Aircraft,* Springer-Verlag, New York, 1990.

[2] Haiges, K. R., Chiang, R. Y., Madden, K. P., Emami-Naeini, A., Anderson, M. R., and Safonov, M. G., "Robust Control Law Development for Modern Aeroscope Vehicles, Final Report," WL-TR-91-3105, Wright Laboratory, Wright-Patterson Air Force Base, OH, Aug. 1991.

[3] Chiang, R. Y., Safonov, M. G., Haiges, K. R., Madden, K. P., and Tekawy, J. A., "A Fixed H_∞ Controller for a Supermaneuverable Fighter Performing a Herbst Maneuver," *Automatica,* Vol. 29, No. 1, 1993, pp. 111–127.

[4] Sparks, A. G., and Banda, S. S., "Application of Structured Singular Value Synthesis to a Fighter Aircraft," *Proceedings of the 1992 American Control Conference* (Chicago, IL), 1992, pp. 1301–1305.

[5] Adams, R. J., Buffington, J. M., Sparks, A. G., and Banda, S. S., "An Introduction to Multivariable Flight Control System Design," WL-TR-92-3110, Wright Laboratory, Wright-Patterson Air Force Base, OH, Oct. 1992.

[6] Bugajski, D. J., and Enns, D. F., "Nonlinear Control Law with Application to High Angle-of-Attack Flight," *Journal of Guidance, Control, and Dynamics,* Vol. 15, No. 3, 1992, pp. 761–767.

[7] Snell, S. A., Enns, D. F., and Garrard, W. L., "Nonlinear Inversion Flight Control for a Supermaneuverable Aircraft," *Journal of Guidance, Control, and Dynamics,* Vol. 15, No. 4, 1992, pp. 976–984.

[8] Huang, C., Knowles, G., Reilly, J., Dayawansa, M., and Levine, W., "Analysis and Simulation of a Nonlinear Control Strategy for High-Angle-of-Attack Maneuvers." 1990 AIAA Guidance, Navigation, and Control Conference, Portland, OR, Aug. 1990.

[9] Durham, W. C., "Constrained Control Allocation," *Proceedings of the 1992 AIAA Guidance, Navigation, and Control Conference* (Hilton-Head, SC), AIAA, Washington, DC, 1992, pp. 1147–1155.

[10] Haiges, K. R., Tich, E. J., and Madden, K. P., "Robust Control Law Development for Modern Aerospace Vehicles, Task 1: Model Development," WRDC-TR-89-3080, Wright Laboratory, Wright-Patterson Air Force Base, OH, Aug. 1989.

[11] Miele, A., *Flight Mechanics: Theory of Flight Paths, Vol 1,* Addison-Wesley, Reading, MA, 1962.

[12] Anon., "Military Specification—Flying Qualities of Piloted Vehicles," MIL-STD-1797A, March 1987.

[13] Slotine, J. E., and Li, W., *Applied Nonlinear Control,* Prentice-Hall, Englewood Cliffs, NJ, 1991.

[14] Lane, S. H., and Stengel, R. F., "Flight Control Design Using Nonlinear Inverse Dynamics," *Automatica,* Vol. 24, 1988, pp. 471–483.

[15] Doyle, J. C., "Analysis of Feedback Systems with Structured Uncertainties," *IEEE Proceedings,* Vol. 129, Part D, No. 6, Nov. 1982, pp. 242–250.

[16] Doyle, J. C., Wall, J., and Stein, G., "Performance and Robustness Analysis for Structured Uncertainty," *Proceedings of the 21st IEEE Conference Decision Contr.,* Orlando, FL, Dec. 1982, pp. 629–636.

[17] Doyle, J. C., "Structured Uncertainty in Control System Design," *Proceedings of the 24th IEEE Conference Decision Contr.* (Ft. Lauderdale, FL), 1985, pp. 260–265.

[18] Balas, G. J., Packard, A. K., Doyle, J. C., Glover, K., and Smith, R., "Development of Advanced Control Design Software for Researchers and Engineers," *Proceedings of the 1991 American Control Conference* (Boston, MA), 1991, pp. 996–1001.

[19] Haiges, K. R., Madden, K. P., and Eller, B. G., "Robust Control Law Development for Modern Aerospace Vehicles, Task 2: Control System Criteria and Specifications," WRDC-TR-90-3005, Wright Laboratory, Wright-Patterson Air Force Base, OH, Aug. 1989.

[20] Buffington, J. M., Adams, R. J., and Banda, S. S., "Robust, Nonlinear, High-Angle-of-Attack Control Design for a Supermaneuverable Vehicle," *Proceedings of the 1993 AIAA Guidance, Navigation, and Control Conference* (Monterey, CA), AIAA, Washington DC, 1993, pp. 690–700.